Case Studies in Thermal Engineering 22 (2020) 100734

Contents lists available at ScienceDirect

Case Studies in Thermal Engineering

journal homepage: http://www.elsevier.com/locate/csite

Optimal cascade phase change regenerator for waste heat recovery in a batch industrial dryer

Gianluca Valenti *, Camilla Nicol Bonacina, Abdullah Bamoshmoosh

Politecnico di Milano, Dipartimento di Energia, Via Lambruschini 4A, 20156, Milano, Italy

ARTICLE INFO

Keywords:
Thermal storage
Industrial laundry
Drying process
Rod bundle regenerator
Fixed bed regenerator

ABSTRACT

Waste heat recovery is one of the main strategies to reduce the use of primary resources. This work develops a cascade phase change regenerator to recover energy from exhaust air to fresh air of a natural gas-fired batch dryer in an existing industrial laundry, taken as a case study, where an experimental campaign is conducted. The regenerator comprises two vertical stoves made of horizontal rod bundles in an aligned configuration to mitigate the fouling. The rods are hollow smooth cylinders that are grouped into sectors, each of which is filled with a phase change material properly selected among paraffins. The number of cylinders per row and the cylinder diameter are investigated by a parametric analysis; the number of sectors and the materials filling each sector are optimized by two alternative algorithms, one based on the process physics and the other on a statistical method. At last, an economic analysis is applied to the optimal configuration. This optimal configuration turns to be an 8-sector regenerator that attains an energy recovered of 61.5% and a net annual saving of 3340 €/year and that requires a total cost of about 9500 €, yielding a payback time lower than 3 years.

1. Introduction

The need for energy is increasing continuously worldwide, posing the global issues of accessing the primary sources while limiting the environmental impacts. In this scenario, the strategies for increasing the energy efficiency in the industrial sector could reduce the primary energy consumption between 18% and 26% [1] and decrease the carbon dioxide emissions by up to 1.8 Gton [2]. Among these strategies, waste heat recovery is considered as one of the most effective.

This work focuses on reducing the energy consumption of a natural gas-fired batch dryer in an industrial laundry by recovering waste heat from exhaust air to fresh air through a cascade phase change regenerator. The regenerator works naturally in a batch mode, so that it follows inherently the intermittent working mode of the dryer itself. The exhaust air from the dryer flows downward in one stove of the regenerator during the hot blow, transferring its energy to the stove bed. On the other hand, the fresh air flows upward in the other stove during the cold blow. The fresh air is consequently preheated by the hot stove bed, reducing thus the consumption of the natural gas in the burner of the dryer. The stove feeds are switched each dryer cycle to alternate the process. Furthermore, each stove bed is made of a horizontal rod bundle in an aligned configuration to mitigate substantially the fouling, which is a severe problem in laundry dryers. The rods of the bundle are hollow smooth cylinders filled with phase change materials that are properly selected. The whole bundle is indeed divided into few sectors with each sector employing one phase change material: at locations closer to the

* Corresponding author.
E-mail address: gianluca.valenti@polimi.it (G. Valenti).

https://doi.org/10.1016/j.csite.2020.100734
Received 1 March 2020; Received in revised form 13 June 2020; Accepted 2 August 2020
Available online 10 August 2020
2214-157X/© 2020 The Author(s). Published by Elsevier Ltd. This is an open access article under the CC BY-NC-ND license (http://creativecommons.org/licenses/by-nc-nd/4.0/).

hot inlet, the material is characterized by a higher phase change temperature than closer to the cold inlet. Fig. 1 shows a schematic of the regenerator made by the two rectangular stove beds each with a bundle of aligned horizontal rods that are filled with phase change materials. The figure indicates also the switching mechanism between the hot and the cold blows; in particular, it shows a hot blow on the left stove, from top to bottom, and a cold blow on the right one, from bottom to top.

Heat exchangers and heat pumps are the most common devices for heat recovery in the dryer industry. Generally, heat exchangers are characterized by inferior recoveries, but they are preferred because of their cost and simplicity [3]. In their turn, heat pumps ensure superior performances, while consuming an amount of electric energy. Jokiniemi et al. [4] study and design a plate heat exchanger obtaining an energy recovery of 18%. Minea [5] performs a theoretical model for a wood-drying heat pump, obtaining recoveries between 42% and 48%. Moreover, combinations of these two technologies are studied by Bisharat and Krokida [6], who predict recoveries up to 40%. These studies consider only continuous processes, whereas works on batch processes appear to be uncommon in the open literature.

Regarding cascade phase change regenerators, recent works are available in the literature. Khor et al. [7] divide a regenerator for cold energy storage in three sectors, obtaining an energy recovery increase above 10% with respect to a single material configuration. Similarly, Michels and Pitz-Pall [8] obtain recovery improvements subdividing a regenerator for solar collector applications in three sectors. Moreover, Yang et al. [9] maximize the energy recovery of a comparable system through the implementation of an analytical optimization algorithm. These cited works show that the implementation of cascade phase change regenerators leads to appreciable increases of the recoveries with minimal increase in the complexity of the system.

The present work is a major continuation of a previous activity [10]. Here, an experimental campaign at an industrial laundry, taken as a case study, is included. The measurements are employed to define a base configuration, which is investigated in a parametric analysis. Moreover, two optimization algorithms for the order of the phase change materials are implemented in the MATLAB and applied to a selected configuration from the parametric analysis to identify an optimal configuration of the cascade phase change regenerator. Lastly, an economic analysis is executed on the optimal configuration to decide its investment feasibility. The next sections describe the measurements, the simulations, the results from parametric, optimization, as well as economic analyses, and ultimately the conclusions.

2. Case study

This section describes the case study of an industrial laundry dryer adopted in this work, outlining the drying process and the measurements performed on the dryer itself.

2.1. Drying process

The case study is a real natural gas-fired batch dryer for cotton flat fabrics, like bed linens or tablecloths, in an existing industrial laundry. The nominal load of the dryer is 85 kg, referred to the dry fabric. The total cycle time is 20–22 min, including loading, drying, cooling, unloading the fabrics, and automatic cleaning of the dryer. The sole drying process lasts 15–17 min, depending on the load and the ambient conditions.

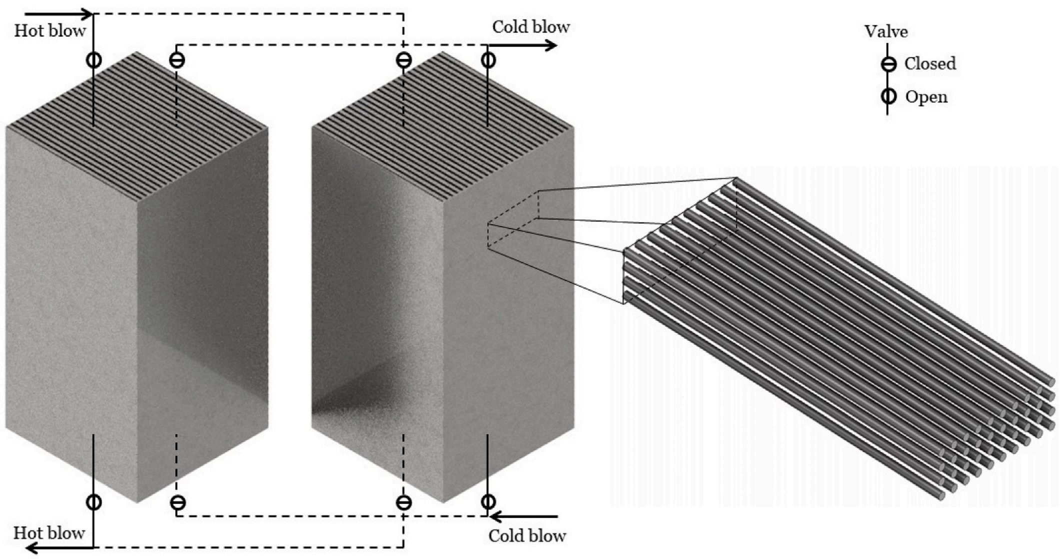

Fig. 1. Schematic of the regenerator made by two stove beds with horizontal rod bundles filled with phase change materials and of the switching mechanisms between hot blow, from top to bottom, and cold blow, from bottom to top.

2.2. Measurements

An experimental campaign is performed to measure the operating conditions of the dryer exhaust air [11]. These measurements represent the inlet conditions of the regenerator during the hot blow. Specifically, its temperature T_{air} (°C) and v_c velocity (m/s) are measured with a mobile hot wire anemometer placed for the campaign in the center of the squared exhaust duct. The drying process is affected by the quantity and the type of the load and, hence, it may change slightly cycle by cycle. Therefore, the measurements are repeated over three cycles for sake of qualitative comparison, but only the last one is taken quantitatively as reference in this work.

From the measurements of exhaust air temperature T_{air} and velocity in the center of the duct v_c during the reference drying cycle, the exhaust air mass flow rate $\dot{m}_{air}$ (kg/s) at each instant is computed as follows [12].

$$\dot{m}_{air} = \rho_{air} v_m A = \frac{M_{air} P_{air}}{\mathscr{R}(T_{air} + 273.15)} v_m L^2 \tag{1}$$

where ρ_{air} (kg/m^3) is the density, while v_m (m/s) the mean velocity of the exhaust air, and A (m^2) the cross section of the squared duct. The density is calculated adopting the ideal gas equation of state and assuming the molar mass M_{air} (kg/kmol) of dry air (as justified at the end of this section), which is equal to 28.9 kg/kmol; moreover, assuming the pressure P_{air} of 100 kPa and the universal gas constant $\mathscr{R}$ of 8314 J/(kmol K). The squared duct side L is 0.5 m. Lastly, the mean velocity v_m is retrieved from the measured velocity at the center of the duct v_c as follows

$$v_m = v_c \frac{2n^2}{(n+1)(2n+1)} \tag{2}$$

where n (−) is a coefficient that depends on the Reynolds number in the center of the duct Re_c (−) according to Ref. [13].

The combined relative uncertainty of the air mass flow rate $u_{\dot{m}_{air}}$ (−), derived according to Ref. [14], turns to be simply as follows [11].

$$u_{\dot{m}_{air}} = \sqrt{{u_{T_{air}}}^2 + {u_{v_m}}^2} \tag{3}$$

where $u_{T_{air}}$ (−) and u_{v_m} (−) are the relative uncertainties of the exhaust air temperature and mean velocity, respectively. The uncertainty on the coefficient n is neglected and, consequently, the relative uncertainty on the mean velocity u_{v_m} (−) turns to be equal to that of the center duct velocity u_{v_c} (−). The relative uncertainty of the mass flow rate during the drying process is between 6% and 10%, with a mean value of 7%, which are rather high values but still acceptable for the scope of this work. Indeed, as anticipated, each cycle is characterized by different operating conditions depending on the type of dried fabrics and the process variability is moderately larger than this relative uncertainties.

Fig. 2 shows the quantities and the uncertainty intervals for the measured temperature and velocity in the center of the duct, while Fig. 3 depicts the calculated mass flow rate of the exhaust air and its combined uncertainty over the reference drying process.

Finally, the absolute humidity is not measured but estimated as the ratio of the mean evaporated water rate from the fabrics and the mean value of the mass flow rate of exhaust air calculated above [11]. The resulting value of the absolute humidity is 0.04 kg$_{water}$/kg$_{dry,air}$, taken constant over the drying process. The use of the absolute humidity in Eq. (1), instead of the assumption of dry air, would lead to a variation of the calculated mass flow rate well below the uncertainty, confirming the validity of the dry air assumption for sake of its density calculation.

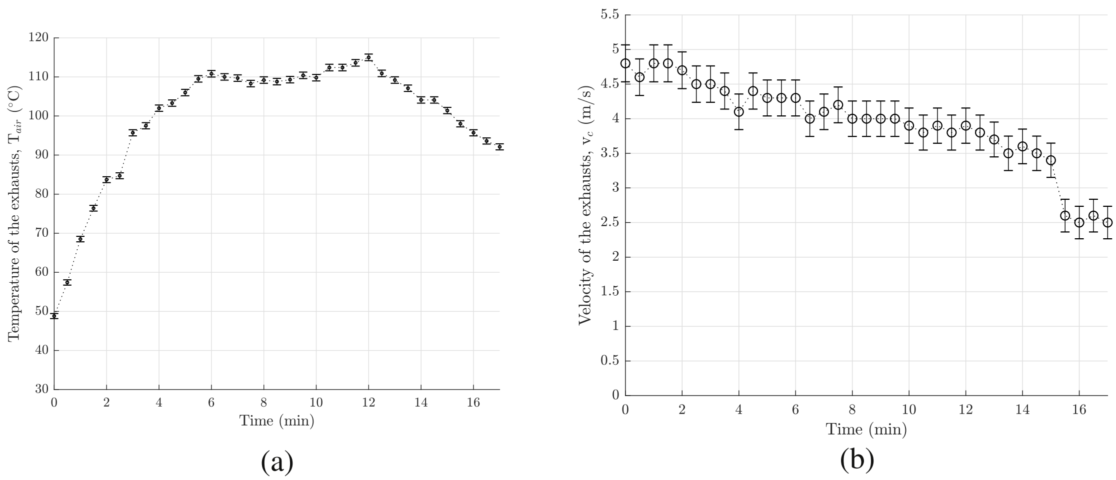

Fig. 2. Quantities and uncertainty intervals of the measured temperature (left) and velocity (right) in the center of the exhaust air squared duct over the reference drying process.

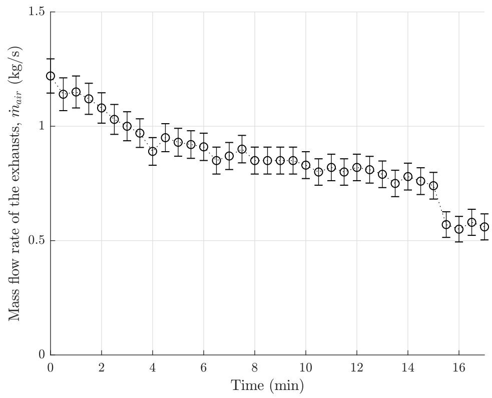

Fig. 3. Quantities and combined uncertainty intervals of the calculated mass flow rate of the exhaust air over the reference drying process.

3. Simulations

This section describes how the simulations are arranged and executed, outlining the process and economic models, the design parameters, two of which are analyzed parametrically, the performance indexes, and the two employed optimization algorithms.

3.1. Process models

Fluid property and heat transfer models are described extensively in the previous work [10]. In summary, ideal gas and incompressible liquid assumptions are used to model the thermodynamic properties and the vapor-liquid equilibria. Moreover, Chung et al. [15] model is used for the transport properties. A global heat transfer coefficient is calculated by the correlations developed by Zukauskas [16] to account for condensation. Moreover, a correction factor is applied to the heat exchange coefficients in the lumped model of the phase change material when the Biot number exceeds 0.1, which may occur likely because of the low conductivity of some phase change materials. In their turn, the pressure drops are calculated via correlations developed by Zukauskas [17] based on the averaged Euler number.

3.2. Economic models

The net annual saving considers both the avoided cost of natural gas in the burner of the dryer due to the energy recovered from the exhaust air to the fresh air by the regenerator as well as the additional cost of the electricity consumed by the fans due to the pressure drops in the regenerator. Thus, the net annual saving C_{save} (€/year) is calculated as follows

$$C_{save} = N_{ccls}\left(\frac{E_{rec}C_{th}}{\eta_{brn}} - 2\frac{E_{pmp}C_{el}}{\eta_{fan}}\right) \tag{4}$$

where N_{ccls} (1/year) is the number of cycles in a year, E_{rec} (J) the energy recovered by the cold blow of a cycle, E_{pmp} (J) the energy consumed by an ideal fan of one stove because of the pressure drops in that stove, multiplied by 2 in the equation since two stoves operate simultaneously, C_{th} and C_{el} (€/J) the thermal and electricity costs, while η_{brn} and η_{fan} (−) the burner and the fan efficiencies, respectively.

Furthermore, the total cost of the regenerator C_{tot} (€) is formulated starting from three main cost items as follows

$$C_{tot} = (C_{PCM} + C_{cln} + C_{csn})(1 + BOP) \tag{5}$$

where C_{PCM} (€), C_{cln} (€) and C_{csn} (€) are the bare equipment costs of the phase change materials, cylinders and casing, respectively. Cylinders and casing are taken to be made of stainless steel because of the possible condensation of the dryer exhaust air. All these bare equipment costs shall be determined from the estimation of the necessary quantity of phase change materials, stainless steel and their specific costs. In particular, the specific costs of cylinders and casing shall account for both the purchased stainless steel and the labor work to manufacture them. The total bare equipment cost is increased by the so-called balance of plant, *BOP* (−), which considers all other cost items not specifically included, such as fans, louvers, ducts, insulation, controller, transportation, and installation.

Ultimately, the simple payback time, *PBT* (year), is computed as the ratio of the total cost of the regenerator and the net annual saving it allows for.

3.3. Design parameters

Each stove of the regenerator is characterized by five main geometrical parameters: frontal area, height, number of cylinders per row, cylinder diameter, and dimensionless vertical pitch. The first variable is set such that the mean velocity in undisturbed conditions of the flow is about 5 m/s, obtaining a frontal area of 0.25 m^2. Thus, considering a squared shape geometry, the width and depth turn out to be 0.5 m, similarly to the squared exhaust air duct of the case study. In its turn, the height is set at the maximum possible value of 3 m due to room limits in the existing laundry of the case study. The number of cylinders per row and their diameter are analyzed parametrically to find the configuration that ensures the highest net annual saving. Lastly, the dimensionless vertical pitch is taken equal to 2 and, then, used to compute the number of rows from the stove height and the cylinder diameter [16].

A market analysis is performed to select the most suitable commercial phase change materials. Among the different types of materials, paraffins are chosen for their easy handling, low corrosiveness and affordable cost. Materials with transition temperature between 40 and 130 °C, which are the operating range of the exhaust air temperature, are selected. Moreover, their flash temperature must be above 200 °C to avoid problems of ignition. Specifically, fourteen commercial paraffins are inserted in the MATLAB database and selected through the optimization algorithms, described below. Table 1 depicts the main properties of the paraffins found on market, where T_{fus} (°C) is the fusion temperature, h_{fus} (kJ/kg) the fusion enthalpy, λ (W/(m K)) the thermal conductivity, c (kJ/(kg K)) the specific heat, ρ (kg/m^3) the density, and T_{flash} (°C) the flash temperature.

3.4. Performance indexes

Three performance indexes are examined in the parametric analysis, out of which two are energy indexes and one is an economic index. The energy indexes are the mass specific recovery (kJ/kg) and the pumping work specific recovery (kJ/kJ), which are the ratios of the energy recovered E_{rec} with respect to the total mass of the stove and to the pumping work E_{pmp}, respectively. In its turn, the economic index is the net annual saving C_{save} as computed in Eq. (4). These indexes are employed to identify a selected configuration, in terms of number of cylinders per row and their diameter, to be optimized, in terms of diverse sectors.

The last index is an energy index that describes the performances of the regenerator. It is the recovery efficiency, expressed as the ratio between the energy recovered by the cold blow E_{rec} and the maximum energy ideally exploitable from the hot blow cooling it to ambient temperature. This index is the objective function of the optimization algorithms that defines the optimal cascade phase change regenerator.

3.5. Two optimization algorithms

Two optimization algorithms are employed to maximize the recovery efficiency by selecting properly the phase change materials. For the purpose, the regenerator is divided arbitrary into sectors of same size, in other words of same number of rows, that may be filled with phase change materials differing sector by sector in order to exploit their latent heat of fusion in the most efficient way. Specifically, materials with decreasing transition temperature are expected to be assigned by the algorithms from the top to the bottom of the regenerator. Materials are numbered in increasing order from that with higher transition temperature to that with lower transition temperature, starting from 1 as shown in Table 1; sectors are referred to by letters, starting from A at the top of the stove. The optimized parameters, which are the materials of each sector, are integers while the process models are nonlinear, yielding an overall system that is a mixed integer nonlinear problem. Two heuristic methods are adopted: the local search and the genetic algorithm. The former is developed for the purpose and it is based on the problem physics, while the latter is taken from MATLAB built-in functions and it is based mainly on a statistical approach.

The local search approach is an iterative procedure in which an initial guess for the set of materials for all sectors is chosen

Table 1
Properties of the fourteen commercial paraffins (NA stands for not available).

Material	T_{fus} (°C)	h_{fus} (kJ/kg)	λ (W/(m K))	c (kJ/(kg K))	ρ (kg/m^3)	T_{flash} (°C)
1	42	140	0.21	2.22	905	250
2	43	280	0.18	2.37	780	250
3	46	155	0.22	2.22	910	250
4	48	230	0.18	2.85	810	250
5	50	190	0.18	2.15	810	250
6	52	220	0.18	2.15	810	250
7	53	155	0.22	2.22	910	250
8	58	215	0.22	2.22	910	250
9	58	240	0.18	2.85	820	200
10	62	205	0.22	2.2	910	250
11	70	225	0.23	2.2	890	250
12	82	170	0.22	2.21	850	250
13	95	260	0.22	2.2	900	300
14	118	285	NA	2.7	1450	200

arbitrarily. The procedure considers a single sector per iteration, starting from the first sector downwards and, once the last sector is reached, restarting from the first one unless a convergence criterion is met. At each iteration, a population is formed for the sector the iteration refers to. This population consists of all materials between a lower and an upper bound, whereas all other sectors are filled with the same material as at the end of the previous iteration. The two bounds are defined by the material with the transition temperature immediately higher than the material in the previous sector and by the material with the transition temperature immediately lower than the material in the subsequent sector. The whole population is simulated and the set yielding the highest recovery efficiency is selected at the end of that iteration. The convergence criterion is the efficiency recovery gain being lower than an arbitrary tolerance. As an example, Fig. 4 shows the formation of the population for the sector D of the regenerator, where each circle represents a whole sector and the number of the material that fills all the rows of the corresponding sector. In the example, sector D is filled with "6", while C with "5" and E with "8". The lower bound is the material "5 − 1", which is "4", while the upper the material "8 + 1", which is "9". Therefore, the materials for sector D span from "4" to "9".

Similarly, the generic algorithm creates a population of set of materials. However, the way this population is formed is different. Indeed, the materials of all the sectors are studied each iteration and the best configuration is found adopting statistical operators and random mutations. The MATLAB function "ga" from the Global Optimization Toolbox is adapted to the present case study.

4. Results and discussion

This section describes and discusses the results from all simulations, presenting first the outcomes from the parametric analysis on the number per cylinders per row and their diameters of a base configuration for a single-sector regenerator, showing then the improvements of a selected configuration from the parametric analysis by the optimization algorithm on multiple sectors, and illustrating lastly the economic analysis of the optimal configuration.

4.1. Parametric analysis of the base configuration

The base configuration of the parametric analysis is a single sector regenerator employing the paraffin "13" from Table 1, which turns to be the one allowing for the highest net annual saving among all. The two parameters varied in the analysis are the number of cylinders per row, from 11 to 27, and the cylinder diameter, from 9 to 18 mm. Fig. 5 depicts the results of the parametric analysis in terms of the pumping work specific recovery as a function of the mass specific recovery at varying numbers of cylinders per row along each curve, on the left, as well as in terms of the net annual saving C_{save} directly as a function of the number of cylinder per row, on the right. Each curve is drawn for one cylinder diameter.

Referring to Fig. 5(a), the higher the pumping work specific recovery and the mass specific recovery are, the better the energy performance is. Thus, a desirable condition falls in the top and right most corner of the diagram. Each actual curve shows a sharp peak. Each peak represents the threshold between the heat transfer and the pressure drop phenomena at a given cylinder diameter. Furthermore, peaks move right- and downward as the diameter decreases. In other words, the smaller the diameter, the better the mass specific recovery but the worst the pumping work specific recovery. Indeed, the larger the number of cylinders per row and the smaller the diameter, the better the heat transfer between the exhaust air and the phase change materials, but the worst the pressure drops across the stove.

Referring to Fig. 5(b), the higher the net annual saving is, the better the economic performance is. Thus, a desirable condition falls in the top most side of the diagram. Each actual curve shows a smooth peak. Each peak represents the best compromise between the avoided cost of natural gas to the burner and the additional cost of the electricity to the fans. Furthermore, peaks move right- and upward as the diameter decreases. In other words, the smaller the diameter, the better the net annual saving at higher cylinders per row.

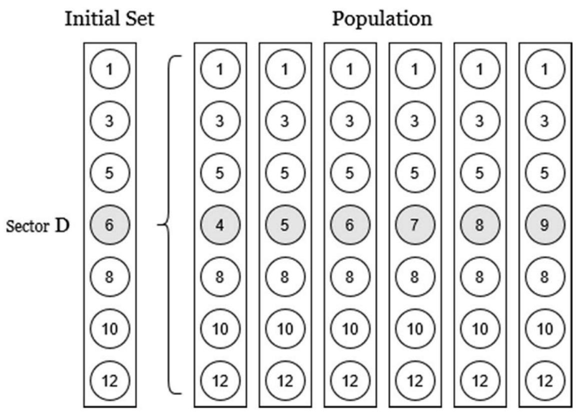

Fig. 4. Example of the formation of a population for the sector D of a 7-sector cascade phase change regenerator: from the initial guess of material "6", a population is generated assigning the materials between the lower bound "4" and the upper bound "9".

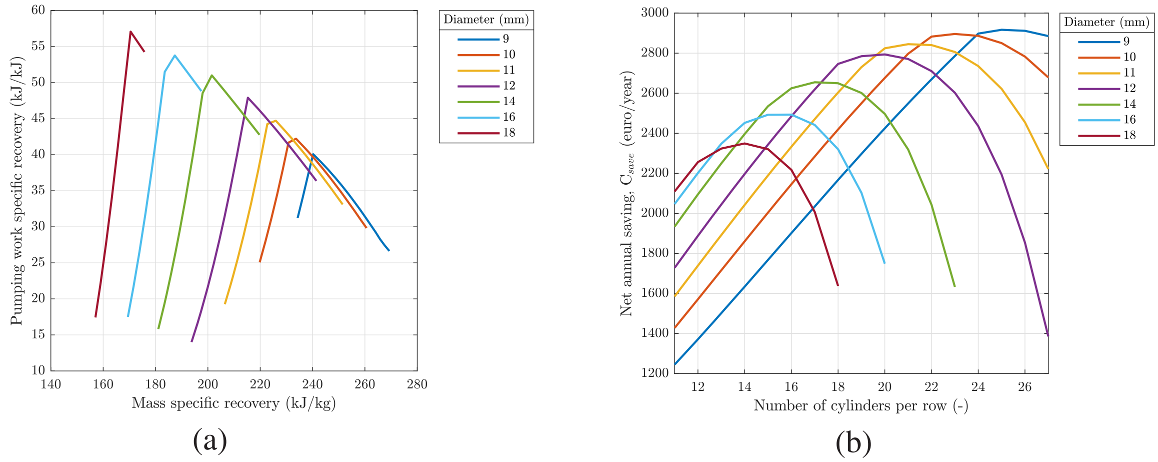

Fig. 5. Results of the parametric analysis on the base configuration in terms the pumping work specific recovery as a function of the mass specific recovery (left) and the net annual saving (right).

Ultimately, the selected configuration among the investigated ones in the parametric analysis comprises 26 cylinders per row with a diameter of 9 mm, resulting in 166 rows per stove and 4316 cylinders per stove.

4.2. Optimization of the selected configuration

Starting from the selected configuration from the parametric analysis, the two optimization algorithms are used to find the optimal configuration with a set of paraffins for a number of sectors ranging from 1 to 10. Adopting the local search algorithm, Fig. 6 shows the energy recovered E_{rec} and the net annual saving C_{save} as a function of the number of sectors achieved by the best set of materials for that number of sectors. The highest energy recovered occur for 4 and 8 sectors, with an increase in the energy recovered and net annual saving of about 10% and 13%, respectively, with respect to the case in which one single-sector is selected. Specifically, the 4 sectors are filled with paraffins "13", "11", "9", "4", while the 8 sectors with "13", "13", "11", "11", "9", "9", "4" and "2" of Table 1, respectively. Results adopting the genetic algorithm are practically equal to Fig. 6 and, hence, they are not reported. However, the local search turns to be usually 2-3 times faster than the genetic algorithm because it is implemented considering the physics behind the problem, rather than operating mainly with a random approach. Ultimately, the optimal configuration is that with 8 sectors.

Fig. 7 shows the temperature distribution during the cold blow of the first, middle and last row cylinders as a function of time, on the left, as well as of the flow as function of the position at different instants, on the right, for the optimal configuration. Referring to Fig. 7(a), plateaus refer to a phase change, while curves at higher temperature to the liquid phase and lower to solid. Hence, the different transition temperatures and the different slopes in the rows highlight the presence of materials with diverse properties along the regenerator. A positive result of this configuration is that all rows undergo the phase change. Moreover, it shows the increasing

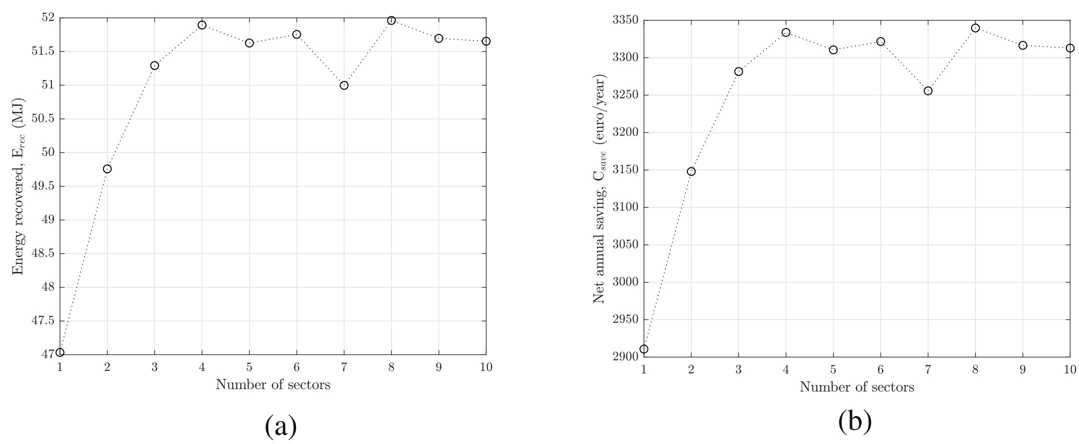

Fig. 6. Energy recovered (left) and net annual saving (right) as a function of the number of sectors of the regenerator for their corresponding best set of materials found with the local search algorithm. Results found with genetic algorithm are practically equal and, hence, not reported.

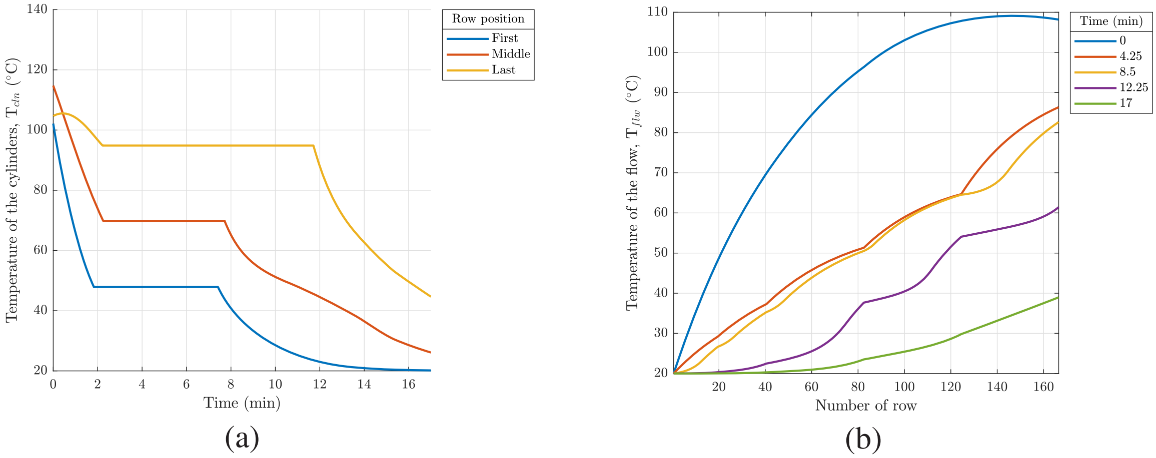

Fig. 7. Temperature distributions during the cold blow of the cylinder temperature for the first, middle and last row over time (left) and the flow temperature across the stove for 5 different instants of the reference drying cycle (right).

time to complete phase change transition between the first and last rows. Referring to Fig. 7(b), curves refer to different instants of the drying process, while inflection points to the interface between two different materials. It shows a continuous decrease of the flow temperature difference from the first (inlet) to the last row (outlet) of the cycle over time. At the beginning, the fresh air is heating by almost 90 °C, whereas at the end by 20 °C. This behavior is due to the decreasing temperature difference between the flow and cylinders corresponding to a decreasing heat transfer.

Overall, the optimal 8-sector configuration leads to a recovery efficiency, recovered and pumping energies of 61.5%, 52 MJ and 1.8 MJ, respectively.

4.3. Economic analysis of the optimal configuration

Table 2 depicts the main parameters used for the economic analysis applied to the optimal configuration. The resulting net annual saving C_{save} is 3340 €/year, as shown in Fig. 6. Moreover, the total mass of phase change materials and steel casing of the two stoves of the regenerator is 230 and 100 kg, respectively. These results are combined with the mass specific costs of phase change materials and steel casing, as well as the cost of the cylinders per meter from Table 2. The bare equipment costs of the phase change materials C_{PCM}, cylinders C_{cln} and casing C_{csn} turn to be 1520 €, 4000 €, and 830 €, respectively. Therefore, the total cost of the regenerator C_{tot} turns to be 9525 € including the balance of plant, which leads to a simple Pay Back Time *PBT* of less than 3 years.

5. Conclusions

This work develops a rod bundle regenerator for waste heat recovery applied to a natural gas-fire batch dryer in an existing industrial laundry, taken as case study, where an experimental campaign is conducted. The rods are hollow smooth cylinders filled with phase change materials. The number of cylinders per row and the cylinder diameters are selected by a parametric analysis. Moreover, the bundle is divided conceptually in sectors, yielding namely a cascade regenerator, and the phase change materials for all sectors are chosen optimally among paraffins by two different algorithms to achieve the maximum energy recovered. Ultimately, an economic analysis is applied to the optimal configuration.

- The literature review indicates that energy recoveries in the industrial dryer industry by heat exchangers and heat pumps can approach 50% and that cascade regenerators can achieve recoveries 10% higher than single-sector ones.
- Measurements of the exhaust air temperature and velocity for a drying cycle are recorded with an anemometer and used to calculate the mass flow rate. The exhaust air from a dryer with a nominal load of 85 kg, referred to the dry fabric, has a temperature varying between 40 and 120 °C, and a rate between 0.5 and 1.25 kg/s. The combined uncertainty on the rate is relatively high, around 7%, but within the process variability over diverse drying cycles.
- The parametric analysis shows that the energy and economic indexes are a compromise between the energy recovered by the regenerator and the fan energy due to the pressure drops through the regenerator itself. Higher number of cylinders per row and smaller cylinder diameters achieve better indexes. For the case study, they are selected 26 cylinder per row with a diameter of 9 mm, resulting in 166 rows over the regenerator height of 3 m.
- Two optimization algorithms, one based on the process physics and the other on a statistical approach, for the choice of the phase change materials are considered. Both algorithms lead to practically identical results. The local search approach, based on the physics, is 2–3 times faster than the genetic algorithm. The optimal cascade configuration is an 8-sector regenerator achieving 13%

Table 2
Parameters for the economic analysis of the optimal configuration.

Parameter	Unit	Value	Parameter	Unit	Value
Cycles per year N_{ccls}	1/year	6000	Cylinder length	mm	500
Cost of electricity C_{el}	€/kWh	0.18	Cylinder diameter	mm	9
Cost of natural gas C_{th}	€/kWh	0.047	Cylinder thickness	mm	1
Fan efficiency η_{fan}	–	0.7	Casing width	mm	550
Burner efficiency η_{brn}	–	0.9	Casing thickness	mm	2
Specific PCM cost	€/kg	6.5	Casing height	mm	3000
Specific cylinder cost	€/m	0.93	Balance of Plant *BOP*	%	50
Specific casing cost	€/kg	8			

higher energy recovered than the single-sector recuperator, in agreement with literature indications, and 61.5% energy recovered, exceeding the literature indications.

- The economic analysis shows that the net annual saving for the optimal configuration is 3340 €/year and that the total cost of the regenerator is about 9500 €, yielding a simple payback time lower than 3 years, which is an interesting result considering current industrial tendencies.

Given the promising results from the economic analysis, the next step of the work is designing in detail the actual optimal cascade phase change regenerator and, eventually, manufacturing as well as testing it.

Credit author statement

Abdullah Bamoshmoosh: software, validation, investigation.
Camilla N. Bonacina: software, validation, investigation, data curation, writing – original draft, visualization.
Gianluca Valenti: term, conceptualization, investigation, writing – review and edit, supervision.

Declaration of competing interest

The authors declare that they have no known competing financial interests or personal relationships that could have appeared to influence the work reported in this paper.

Acknowledgement

The authors acknowledge gratefully Lavanderia Borromeo S.r.l. for giving the opportunity and the time to record the measurements and to discuss the results.

Nomenclature

Acronyms

NA	Not available
PBT	Payback time
PCM	Phase change material
BOP	Balance of the plant

Symbols

η	Efficiency (−)
λ	Thermal conductivity (W/(m K))
ρ	Density (kg/m^3)
A	Area (m^2)
C	Cost (€), specific cost (€/J), and annual saving (€/year)
c	Specific heat (J/(kg K))
E	Energy (J)
f	Generic function
h	Specific enthalpy (J/kg)
M	Molar mass (kg/kmol)
$\dot{m}$	Mass flow rate (kg/s)
n	Generic coefficient (−)
n_{par}	Number of parameters (−)
L	Side length (m)

N	Generic number (−)
P	Pressure (Pa)
R_e	Reynolds number (−)
$\mathscr{R}$	Universal gas constant, 8314 J/(kmol K)
M	Molar mass (kg/kmol)
T	Temperature (K)
U	Uncertainty
u	Relative uncertainty (−)
v	Velocity (m/s)
x	Generic variable

Subscripts

air	Air
brn	Burner
c	Center
ccls	Cycles
cln	Cylinder
csn	Casing
el	Electric
flw	Flow
fus	Fusion
m	Mean
pmp	Pumping
rec	Recovered
save	Saving
th	Thermal
tot	Total

References

[1] International Energy Agency, Tracking Industrial Energy Efficiency and CO2 Emissions, 2007.
[2] F. Kesicki, A. Yanagisawa, Modelling the potential for industrial energy efficiency in IEA's World Energy Outlook, Open J. Energy Effic. 8 (2015) 155–169.
[3] A. Jan-Olof, W. Lars, Improved energy efficiency in sawmill drying system, Appl. Therm. Eng. 113 (2013) 891–901.
[4] J. Tapani, H. Mikko, O. Timo, A. Jukka, Parallel plate heat exchanger for heat energy recovery in a farm grain dryer, Dry. Technol. 34 (5) (2016) 547–556.
[5] V. Minea, Efficient energy recovery with wood drying heat pumps, Dry. Technol. 30 (14) (2012) 1630–1643.
[6] G.I. Bisharat, M.K. Krokida, Heat recovery from dryer exhaust air 22 (7) (2004) 1661–1674.
[7] J. Khor, Y. Li, A. Romagnoli, Packed bed regenerators using cascaded phase change materials: overcharging and possible solutions, in: Proceedings of 13th Conference on Sustainable Development of Energy, Water and Environment Systems, 2018.
[8] H. Michels, R. Pitz-Paal, Cascaded latent heat storage for parabolic trough solar power plants, Sol. Energy 81 (2007) 829–837.
[9] X. Yang, Y. He, Y. Li, H. Song, Exergy analysis and optimization of charging discharging processes of latent heat thermal energy storage system with three phase change materials, Sol. Energy 123 (2016) 206–216.
[10] G. Valenti, A. Seveso, C.N. Bonacina, A. Bamoshmoosh, Assessment of a phase change regenerator for batch industrial dryers, in: 74° Congresso Nazionale ATI, Modena, 2019.
[11] G. Valenti, C. N. Bonacina and A. Bamoshmoosh, "Measured and Derived Data at the Exhaust of a Batch Dryer," Data in Brief, Submitted.
[12] F.P. Incropera, D.P. Dewitt, T. Bergman, A.S. Lavine, Fundamentals of Heat and Mass Transfer, John Wiley & Sons, U.S.A., 2006.
[13] C. Fang, An Introduction to Fluid Mechanics, Springer, Switzerland, 2019.
[14] E.O. Doebelin, Strumenti e metodi di misura, McGraw-Hill Companies, Milano, 2008.
[15] T.-H. Chung, M. Aljan, L.L. Lee, K.E. Starling, Generalized multiparameter correlation for nonpolar and polar fluid transport properties, Ind. Eng. Chem. Res. 27 (1988) 671–680.
[16] A. Zukauskas, Heat transfer from tubes in crossflow, Adv. Heat Tran. 18 (1987) 87–159.
[17] A. Zukauskas, Banks of Plain and Finned Tubes, in: E.U. Schlunder (Ed.), H.E.D.H, 1983.